Journal of Applied Polymer Science

WILEY

Applied Polymer SCIENCE

RESEARCH ARTICLE

Stimuli-Responsive Amino Acid Based Polymeric Nanomicelles With Antimicrobial and Anticancer Activities

Debasrita Bharatiya[1] | Biswajit Parhi[2] | Khumukcham Saratchandra Singh[3] | Bramanandam Manavathi[3] | Pradip Paik[4]

[1]School of Engineering Sciences and Technology, University of Hyderabad, Hyderabad, India | [2]Department of Chemistry, Indian Institute of Science Education and Research, Bhopal, India | [3]Department of Biochemistry, School of Life Science, University of Hyderabad, Hyderabad, India | [4]School of Biomedical Engineering, Indian Institute of Technology (IIT)-BHU, Varanasi, India

Correspondence: Pradip Paik (paik.bme@iitbhu.ac.in; pradip.paik@gmail.com)

Received: 16 August 2024 | **Revised:** 6 October 2024 | **Accepted:** 6 November 2024

Funding: This work was supported by DST-Nanomission, India (Ref: SR/NM/NS-1005/2015), Science and Engineering Research Board, India (Ref: EEQ/2016/000040 and CRG/2023/005576), India, I-DAPT foundation (Ref. I-DAPT/IT (BHU)/2023-24/ Project Sanction/47), STARS-IISc. Bangalore (Ref. MoE-STARS/STARS-2/2023-0318), ICMR (Ref. IIPR-2023-4724/F1), and Seed grants (OH-35) supported by Indian Institute of Technology (BHU), to Prof. Paik. Debasrita Bharatiya acknowledges UGC New Delhi, India for providing fellowship and Rutuparna Jena for her assistance in performing the experiments.

ABSTRACT

Herein this work, a biocompatible polymer synthesis approach has been established for the designing of α-methoxy-ω-amino poly(ethylene glycol)-L-glutamate-L-aspartate [MeO-PEG-NH-*b*-(L-GluA)$_5$-*b*-(L-AspA)$_{18}$]/[PEG-*b*-PBLG-*b*-PBLA] triblock copolymeric nanomicelles by using α-methoxy-ω-amino PEG as a macro initiator via modified ring-opening polymerization. The colloidal stability, remarkable protein folding properties, and distinct morphology of the prepared polymer are confirmed. The microscopic analysis confirms the formation of nanomicelles with an average diameter of 13 nm to 22 nm for [PEG-*b*-PBLG-*b*-PBLA] and [PEG-*b*-PBLG], respectively. The copolymers show an effective influence on self-assembly behavior with respect to change in temperature and pH. The cellular inhibition properties of the block copolymeric micelles is confirmed through in vitro study against the MDA-MB-231 cancer cells. The calculated IC$_{50}$ values for [PEG-b-PBLG] and [PEG-*b*-PBLG-*b*-PBLA] copolymers are found to be 560.340 ± 34.107 μg/mL and 750.468 ± 47.312 μg/mL, respectively. The minimum inhibitory concentration (MIC) for antibacterial activity is calculated to be 0.8 μg /mL against *gram* (−) *Escherichia coli* (*E. coli*) of triblock copolymer. Therefore, the attachment of a new amino acid block in the [PEG-*b*-PBLG-*b*-PBLA] copolymer enhances the thermal stability, protein folding properties, colloidal stability, antibacterial activities, and biocompatibility, on account of which the synthesized triblock copolymer nanomicelle could be beneficial for antimicrobial and anticancer activities.

1 | Introduction

Nano and micro-sized polymeric systems have widely been used in medical technology, packaged items, therapeutics, biosensors, and diagnostics platforms [1–3]. At present, polymer nanoparticles possess increasing demands in the emerging pharmaceutical technology to overcome unsatisfactory challenges with their stimuli-responsive nature, self-assembled behavior, unique morphology and size flexibility, amphiphilicity, compatible functional groups, artificial protein synthesis techniques, and for various therapeutic applications [4]. Further, the self-assembled smart polymeric nanomaterials are also used as potential drug carriers for targeted therapy, as scaffolds for tissue engineering, stents, catheters, drug delivery, cell mimics, nanoreactors, artificial organelles, etc. [5]. The targeted, controlled and sustained drug release activity is seen to be proactive in polymeric amino acids [6]. These polymers are unique in the development of therapeutic formulations.

On the other hand, the hydrophilicity dependant slow degradation rates, good biocompatibility, amphiphilicity, and flexible physico-chemical modifications of polymers, such as poly(amino acid)s (PAAs), glutamic acid (L-GluA), and aspartic acids (L-AspA) are extensively used in making the chemotherapeutics formulation to achieve targeted delivery [7, 8]. The significance of amphiphilic polymers has been verified through the presence of hydrophobic and hydrophilic core@shell structures, where core hydrophobic groups help in the solubilization of hydrophobic drugs through electrostatic interactions and hydrogen bonding, whereas the external hydrophilic shell improves the biocompatibility and other bio-physiochemical stability [9]. These smart polymers exhibit more advantages over low molecular weight polymers and interestingly they quickly show responsive behavior toward pH, temperature, solvent system, and reaction time. The distinct activities of polyglycol especially poly(ethylene glycol) (PEG) such as low protein folding and low immunogenicity make it an effective medium for polymeric delivery systems [10]. The ring-opening polymerization (ROP) between hydrophilic polymer of poly(ethylene glycol) (PEG) and essential amino acids such as (L-GluA), (L-AspA), L-lactide, L-phenylalanine (LPPhe) are found to be useful for drug delivery applications for the treatment of different diseases [11]. It is reported that amphiphilic anionic polymer nano vehicle methoxy poly(ethylene glycol)-b-poly (L-glutamic acid-co-L-phenylalanine) (mPEG-b-P[Glu-co-Phe]), which can bind with cationic anticancer drug doxorubicin hydrochloride (DOX.HCl) due to the electrostatic interactions and is found to be effective for the inhibition of cancer cells. The 140 nm-sized DOXmPEG-b-P(Glu-co-Phe) nanoparticles (DOX-NP) show low to moderate drug-loading capacity [12]. The presence of functional groups such as -COOH, -NH_2, -OH, and -SH and the chemical bonding play important role in improving the amphiphilicity of polymers. Further, the morphological pattern also affects the efficacy of self-assembled polymer in in vivo imaging and drug delivery [13]. The dual thermoresponsive nature of mPEG-b-poly(O-benzyl-L-threonine acid) hydrogel and their detailed secondary structure also possesses an important role in therapy due to the self-assembly, stimuli-responsive nature of precursor PEG [14]. The chemical and physical properties of the stimuli-responsive polymeric vesicles and their effects on the controlled release of the drugs are very interesting in controlling the therapeutic doses [15]. Further, the thermo-responsive nature of the polymers to the size and shape affect the bactericidal to cell repellency [16]. In another study, it was reported that an amphiphilic poly(l-glutamic acid)-block-poly(lactic-co-glycolic acid) copolymers designed to control the self-assemble activity at different stimuli and used in the biological systems together with potential therapeutic efficacy [17], which also influence for the new design of the polymers for better therapeutic index. To note, there are many reports available for the synthesis of self-assembled di-block/tri-block-copolymers that possess pH and temperature-responsive nature using two to three identical or nonidentical monomers [18, 19]. To the best of our knowledge, only a few reports are available with three or more distinct monomer units to form synthetic block-copolymers with a wide range of biological applications. Therefore, there is a lot of scope to explore in the domain.

It can be noted that for the preparation of PEG@Polyaminoacids, (PEG@PAAs) polymers has been extensively reported with their detailed physio-chemical properties [9, 14]. However, their stimuli-responsive study in an aqueous medium is quite challenging. Notably, the integration of a new block copolymer has been garnered significant interest in finely adjusting the morphological and biological features with improved surface stability [10]. Therefore, we aimed to identify a novel strategy that would allow proper analysis of prepared polymer at different stimuli, which further can be used as antimicrobial agents. To achieve this, we have investigated the responses of the synthesized polymers at different pH, temperature, and concentration. We have earlier reported a diblock copolymer [PEG-*b*-PBLG] with its various characteristic properties [20], however, a detailed study on folding, morphology, versatile biological applications, and size variation with adverse effects such as pH and temperature have never been reported.

Herein this work, we have investigated the stability of the polymeric solution in a colloidal medium, protein folding nature, morphology, and antimicrobial efficacy resulting in the prepared micelles in a better organized morphology compared to similar conventional polymers. Together with the many advantages of micelles, many more challenges to increasing therapeutic efficiency have been studied. From our earlier study, it is observed that the use of PEG/PAAs as a block of the block copolymer made it promising for various biomedical applications. However, there is no work reported for the design of [(MeO-PEG-NH)-*b*-(L-GluA)-*b*-(L-AspA)] via modified ring opening polymerization (ROP) and its detailed stimuli responsive attribute. The colloidal properties, smart self-assembly behavior, temperature and pH-dependent stimuli-responsive behavior, formation of minute-sized micellar morphology, and thermal stability of the polymers have been studied. Herein, we have taken the amino acid chains as the primary backbone of the polymer due to its unique nature, colloidal properties, and biocompatible nature, which further can be used for various pharmaceutical and medical applications [21, 22]. The morphological features of these types of polymers can further exhibit significant physio-chemical behavior [23, 24]. Polymeric micelles of diameter ~10 nm synthesized in this work can be used as a drug delivery vehicle for the targeted therapy and other biomedical applications including as an antimicrobial agent. The present work is extended to find out the protein folding nature with change in the pH (from 4 to 10) and with temperature (from 20°C-50°C). Secondary folding structures have been analyzed using Circular dichroism (CD). Then we studied the biocompatibility of the synthesized polymers through MTT assay. Finally, the antibacterial activities of the synthesized polymer micelles have been investigated using gram (+) *S. aureus* and gram (–) *E. coli* with varying concentrations of copolymers to calculate the MIC. Further, the therapeutic efficiency and the mechanistic approach of inhibition have been elucidated. Finally, in vitro anticancer activity of these micelles has been checked against triple negative breast cancer cell lines (MDA-MB-231).

2 | Experimental Section

2.1 | Materials

Commercially available reagents were used without further purification. They are Triphosgene (> 99.9%, Sigma-Aldrich), L-glutamic acid-γ- benzyl ester (> 98%, Sigma-Aldrich), L-aspartic acid-β-benzyl ester (> 98%, Sigma-Aldrich), α-methoxy-ω-amino-PEG

(> 98.5%, Iris Biotech GmbH, Germany, 5000 Da), tetrahydrofuran (THF) (> 99%, FINAR), ethyl acetate (> 99%, FINAR), sodium bicarbonate ($NaHCO_3$) (> 98.5%, SRL), petroleum ether (> 98.9%, SRL), palladium activated carbon charcoal (10%) (> 99.9%, Sigma-Aldrich), methanol (> 99%, FINAR), ethanol (> 99%, FINAR), phosphotungstic acid (> 93.8%, Sigma-Aldrich), acetone (> 96%, Sigma-Aldrich), ethanol (> 97.9%, Merck), Na metal (> 99.9%, Sigma-Aldrich, dipped in mineral oil), $CDCl_3$ (> 99.9%, FINAR), benzophenone (> 99.9%, Sigma-Aldrich), potassium bromide (> 99.9%, Sigma-Aldrich), Rhodamine 6G (Sigma-Aldrich), DDI water filter (< 5 nm mesh size).

2.2 | Synthesis of a Triblock Copolymer of [PEG-*b*-PBLG-*b*-PBLA]

2.2.1 | Synthesis of NCA BLG and NCA BLA

In brief, a solution of triphosgene (2.5 g, 0.0043 mol) and dry THF (50 mL) was added separately to a milky white solution of L-glutamic acid γ-benzyl ester (4 g, 0.0085 mol) and dry THF (50 mL) in round bottom 1 (RB1) and L-aspartic acid-β-benzyl ester (4.2 g) and dry THF (50 mL) in RB2. The reactions were carried out in an inert atmosphere as the reducing agent and solvent medium are very sensitive to moisture. The mixtures were continuously stirred for 4 h at 50°C and after the initial step was completed, the product formation was collected in the form of a clear solution. Purification of NCAs was done by evaporation followed by crystallization and recrystallization methods with the use of solvent mixture of 1:1 hexane:THF. The yield of NCA BLG was 3 g (75%) and for NCA BLA is 3.2 g (80%). (Scheme 1, Step 1 (i) and (ii)).

2.2.2 | Synthesis of Dehydrogenated Diblock Copolymer [PEG-b-BLG]

The synthesis method for [PEG-*b*-PBLG] diblock polymer was followed in detail as reported in our earlier work [20]. In short, PEG was added to a solution of NCA BLG and performed the reaction till it produced a shiny pale-yellow solid in an inert atmosphere. (Scheme 1, Step 2).

2.2.3 | Synthesis of a Triblock Copolymer of [PEG-b-PBLG-b-PBLA]

This method involves the conversion of acid to anhydride with the help of a reducing agent triphosgene which is highly hygroscopic. PEG was added to a solution of an NCA BLG and allowed reaction till it produced a shiny pale yellow solid. Then we added the dissolved solution of NCA BLA with dry THF to the [PEG-*b*-BLG] solution. The reaction mixture turned into a transparent solution after the addition of NCA BLA. The reaction mixture was again allowed to be stirred properly for 72 h at 600 RPM and 40°C with an inert atmosphere until the completion of the reaction (Scheme 1, Step 3). Here the formation of benzylated triblock copolymer [PEG-*b*-BLG-*b*-BLA] was syntheiszed. After the completion of the reaction, the mixture was evaporated and purified through the recrystallization method (hexane and THF, 1:1). Then hydrogenation was performed using Pd-C, H_2/THF to obtain the final block copolymer (Scheme 1, Step 4). The synthesized product was collected and allowed for freeze-drying. The detailed synthesis scheme is shown in Scheme 1 and filed for Indian patent Ref. Application No.: 202011029248, (9th, July 2020).

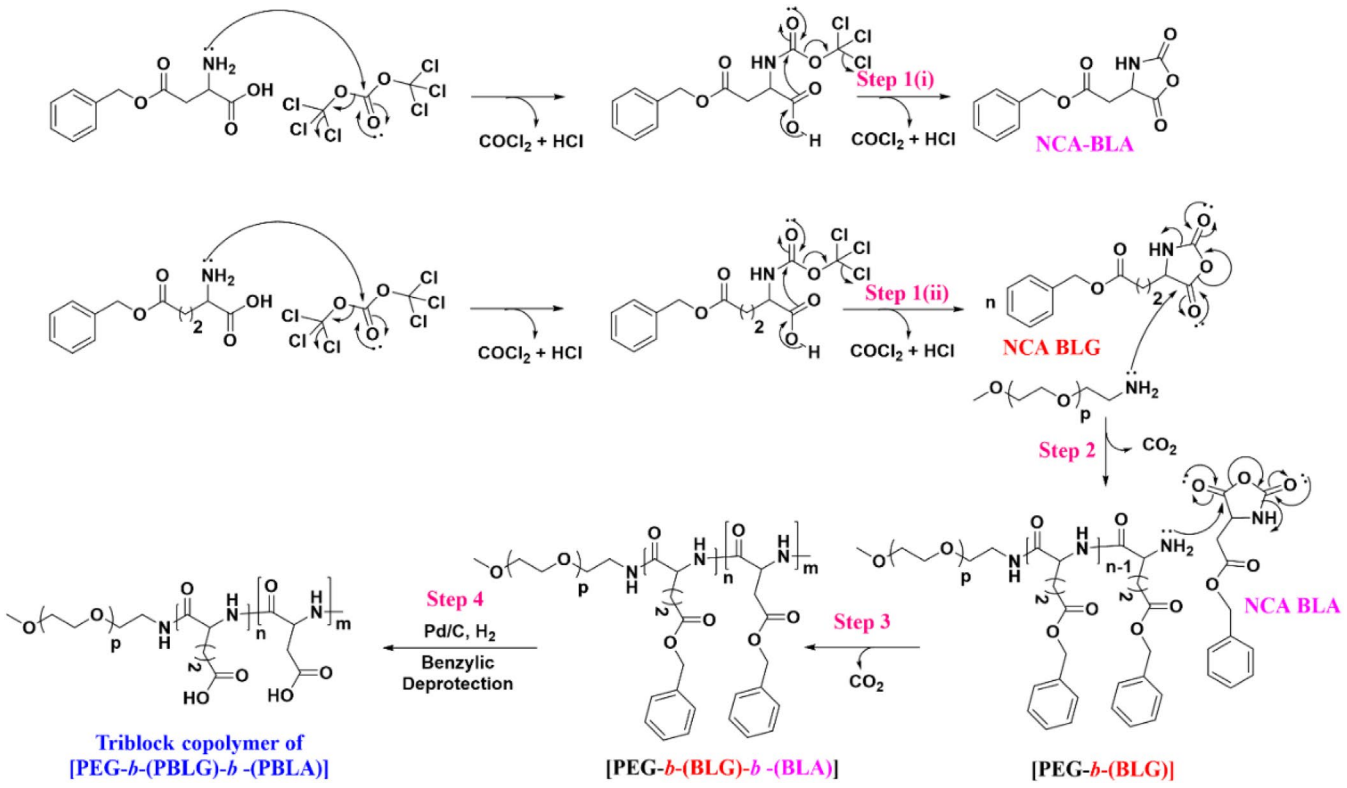

SCHEME 1 | Show the mechanistic pathway involved in the synthesis approach of [PEG-*b*-PBLG-*b*-PBLA] copolymers through ring-opening polymerization. [Color figure can be viewed at wileyonlinelibrary.com]

2.2.4 | In Vitro Cell Maintenance for Cytotoxicity Assay Test

The methyl thiazolyl tetrazolium (MTT) assay was used for the biocompatibility test of the above polymeric micelles using MDA-MB-231 cell lines (obtained from the National Centre for Cell Science (NCCS), Pune, India). Cells were cultured in Dulbecco's Modified Eagle medium (DMEM) supplemented with 10% heat-inactivated fetal bovine serum (FBS), 100 units/mL penicillin, 100 μg/mL streptomycin and cultured at 37°C, 5% CO_2 humidified incubator. Details of the methods have been followed as per our previous reports [23, 25].

2.2.5 | Antibacterial Activities Studies Against Different Bacterial Models

In vitro, antibacterial susceptibilities of polymeric micelles were investigated by the broth dilution method using two microorganisms, for example, gram-negative *ATCC bacterial strains of E. coli* (*ATCC-25922*) and gram-positive *S. aureus* (*ATCC-25923*). The bacterial strains were taken and incubated at 4°C. Briefly, 5 μL of the bacterial culture in each segment of 96-well plate followed by 150 μL of broth containing 50 μL different concentrations (1.25 mg mL^{-1} with serial dilution up to 0.0048 mg mL^{-1}) of samples [PEG-*b*-PBLG] and [PEG-*b*-PBLG-*b*-PBLA], and incubated for 24 h at a physiological temperature (37°C) for both the bacterial strains. The last segment was the tenth segment consisting of bacterial stains but without any sample medium. We have studied the antibacterial activities of polymeric micelles with different types of bacteria and have found the effectiveness of our materials for further biomedical applications. All the samples were characterized by suitable methods.

2.3 | Characterization Techniques

The solid-state crystal structure of synthesized polymers was studied through XRD in the range of $2\theta = 10\text{-}60^{o}$ by a Bruker AXS Model D8 Advanced X-Ray Diffractometer. The thermal stabilities were studied through TGA (Thermo ONIXSGaslab 300). Morphology, size, and elemental composition of the polymer were performed by FESEM (Model: ZEISS Ultra) and the SAED patterns by using TEM (Model FEI Technai G2 200 S–Twin). Surface chemical structure and functional groups were investigated with an FT-IR (Nicolet model impact-410) by making KBr pellets. Chemical structures were confirmed through a ^{1}HNMR model no Bruker DPX ^{1}HNMR (400 MHz) (Ultra Shield). DLS and ZETA analysis was performed through the Malvern 922,008 instrument to give size distribution intensity along with potential raised on the interface of the particles. The physical structure and protein folding of the synthesized polymers were studied through a CD (JASCO Corp., J-810). UV–Vis absorption of the samples was studied through a UV–Vis–NIR spectrometer (LAMDA 750 spectrometer, PerkinElmer). The molecular weight (Mw) of the synthesized polymers was confirmed through MALDI-TOF (model MALDI TOF/TOF-Autoflex III smart beam, Bruker Daltonics). Laser imaging of micelles was performed using the confocal microscope Zeiss LSM 700. MTT assay and antibacterial study were performed by using a Multimode reader (iMark Microplate Absorbance Reader, Bio-Red) and using Infinite 200 PRO NanoQuant, and TECAN spectrometer, respectively.

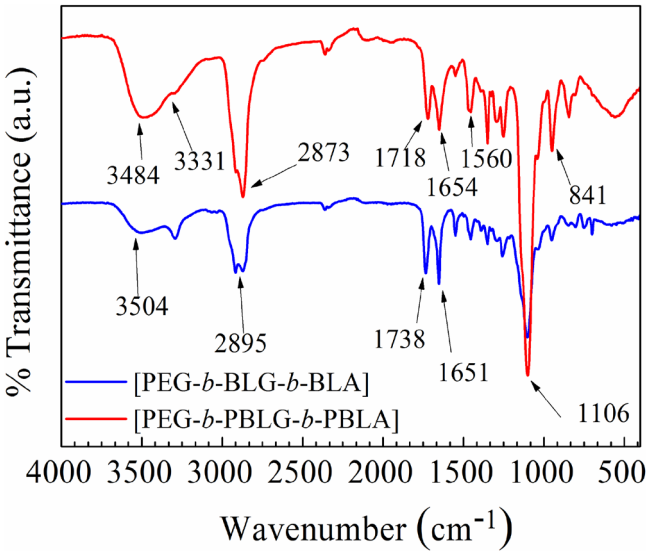

FIGURE 1 | FTIR spectra of [PEG-*b*-BLG-*b*-BLA] and [PEG-*b*-PBLG-*b*-PBLA] copolymers. [Color figure can be viewed at wileyonlinelibrary.com]

3 | Results and Discussion

3.1 | Physical and Chemical Characterization

The identification of chemical functional groups of the designed polymer was studied through FTIR spectroscopy. Figure 1 shows important bands at 1651 cm^{-1} (for amide I, -$CONH_2$), 1545 cm^{-1} (for amide II, -CONH-), and 1738 cm^{-1} (for benzyl ester, C=O) for [PEG-*b*-BLG-*b*-BLA]. This spectra also shows the characteristic bands at 3484 cm^{-1} (O-H str of terminal acid), 3331 cm^{-1} (N-H str), 2873 cm^{-1} (C-H str of –CH_2 units), 1718 cm^{-1} (-COOH group), 1654 (amide, C=O), 1560 cm^{-1} (2° amide), 1466 cm^{-1} (C-H bending) in methylene group and 841 cm^{-1} (-CH_2 rocking) for [PEG-*b*-PBLG-*b*-PBLA] polymer. The band appeared at 1718 cm^{-1} is attributed to -COOH of amino acid-based aspartic acid and glutamic acid in the [PEG-*b*-PBLG-*b*-PBLA] copolymer [22]. This is a strong evidence for the formation of benzylated free [PEG-*b*-PBLG-*b*-PBLA] triblock copolymer with the disappearance of benzylated ester band in [PEG-*b*-BLG-*b*-BLA] polymer at 1738 cm^{-1} after catalytic hydrogenation [26]. The presence of an absorption band at 1651 cm^{-1} is due to the α-helical structure which further has been confirmed through a CD spectroscopy study [20]. For the newly synthesized triblock copolymer [PEG-*b*-PBLG-*b*-PBLA], after catalytic hydrogenation it exhibits a more intense band in FTIR spectra than [PEG-*b*-BLG-*b*-BLA] polymer, introducing an additional number of functional groups. Further, the FTIR spectra confirmed the presence of pure triblock copolymer with targeted functional groups like amide, carboxylic, hydroxyl, and C-N groups for targeted delivery.

The ^{1}HNMR study provides a strong interpretation of the positioning of hydrogens in the polymer. Different types of protons situated in the designed polymer are studied by ^{1}H NMR (500 MHz, $CDCl_3$). Figure 2a represents the ^{1}HNMR analysis for

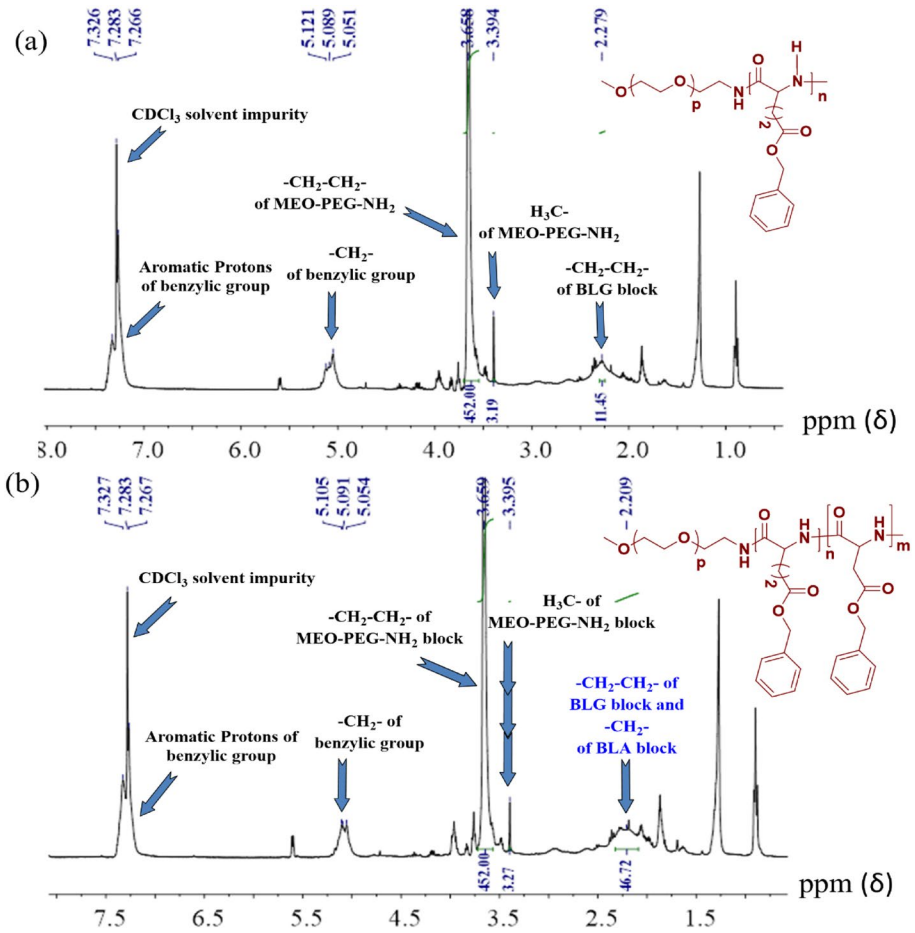

FIGURE 2 | (a) and (b) ^{1}H NMR results obtained for [PEG-*b*-BLG] and [PEG-*b*-BLG-*b*-BLA] copolymers, respectively using $CDCl_3$ as solvent. Where, p = no. of CH_2 units of PEG, n = no. of CH_2 units of glutamate and m = no. of CH_2 units of aspartate (NMR 500 MHz, $CDCl_3$). [Color figure can be viewed at wileyonlinelibrary.com]

[PEG-*b*-BLG_5] copolymer before catalytic hydrogenation, confirming the presence of $n = 5$ number of glutamic CH_2– units in the linear backbone of (MeO-PEG-NH_2). The presence of 5 -CH_2 units was also verified and confirmed through the MALDI-TOF [17, 25, 26]. The ^{1}HNMR δ values for [PEG-*b*-BLG_5] copolymer are as follows: $\delta = 7.32$ (5H, an aromatic proton of $(BLG)_5$), $\delta = 7.26$ ($CDCl_3$), $\delta = 5.08$ (Ar-CH_2-), $\delta = 3.66$ (452H, CH_2 group of MEO-PEG-NH_2), $\delta = 3.4$, (-OCH_3), $\delta = 3.1$, (CH_2 alpha to C-N bond), $\delta = 2.26$ (11H, CH_2 group $(BLG)_5$), and $\delta = 1.9$ (3H, -CH_3). The addition of the third block, that is, NCA BLA to [PEG-*b*-BLG], causes the increment of $m = 18$ number of –CH_2 units, making a total number of 46 –CH_2 units showing a significant band at $\delta = 2.3$ (see in Figure 2b). This also provides information about the additional 10 -CH_2 units in the amide backbone of diblock and the other proton active bands present at $\delta = 7.33$ (12H, an aromatic proton of glutamic acid and aspartic acid with $CDCl_3$), $\delta = 5.603$ (3H, a benzylic proton), $\delta = 3.7$ (452H, -CH_2 group of MEO-PEG-NH_2), and $\delta = 2.261$ (46H, -CH_2 group of glutamic acid, and aspartic acid). The synthesized benzylated triblock copolymer [PEG-*b*-BLG_5-*b*-BLA_{18}] is showing a shift of -CH_2 from $\delta = 2.279$ to 2.209 due to the shielding effect caused by the greater number of proton signals toward TMS. Figure S1 represents the near-view cross-sectional NMR data of nonbenzylated [PEG-*b*-PBLG] and [PEG-PBLG-PBLA] after catalytic hydrogenation. This graph seems to possess similar NMR bands to [PEG-*b*-BLG], however, this indicates the absence of benzyl protons in it. This study also suggests the loss of the -CH_2-CH_2- group of MeO-PEG-NH_2 block in [PEG-*b*-BLG] diblock copolymer, whereas no such loss is noticed in case of [PEG-PBLG-PBLA] triblock copolymer. This retention of -CH_2-CH_2- groups of PEG block in the triblock copolymer can be attributed to the intramolecular hydrogen bonding between -COOH groups of BLG and BLA blocks. This phenomenon causes the unavailability of acidic proton for the degradation of the -CH_2-CH_2 part of PEG in [PEG-PBLG-PBLA] copolymer. Thus, the ^{1}HNMR study confirms that the amino acid-based NCA BLA groups are attached to the backbone of [PEG-*b*-BLG] polymer successfully. This result is promising in controlling the folding behavior of the synthesized copolymers that have been explained in the subsequent section through the CD study.

MALDI-TOF gives information about the M_w of the prepared polymer. Figure 3 illustrates the M_w of [PEG-*b*-BLG_5-*b*-BLA_{18}] copolymer. Figures S2a and S2b represent the M_w results obtained from MALDI-TOF for NCA BLG and [PEG-*b*-BLG] diblock copolymer before catalytic hydrogenation. In this work, the macro initiator used is α-methoxy-ω-amino-PEG with M_w of 5000 Da. The M_w of [PEG-*b*-BLG-*b*-BLA] triblock polymer after polymerization is found to be 10,331 Da. The theoretical mass of the second repeat unit NCA-BLG (γ-benzyl L-glutamate) is 263 g/mol. From Figure S2a, the M_w of the second block is found to be 1503 g/mol. After the polymerization of [PEG-*b*-BLG] diblock

copolymer, M_w is found to be 5812 g/mol. This study suggests that 5 units of glutamate have been attached as di-block to α-methoxy-ω-amino-PEG. This study also gives an idea that, after diblock polymerization, the M_w of α-methoxy-ω-amino-PEG became 4301 g/mol. The degradation of -CH_2-CH_2- in PEG occurs due to the absence of intra-molecular H-bonding that analyzed from ^{1}HNMR spectra. Figure 3 further shows the stepwise addition of monomers and the increment of the M_w concerning the band intensity of the starting material. In the previous reports, it was explained that with the addition of new blocks, the M_w of the new polymer can be increased through various methods such as ROP, addition, condensation, and step growth polymerization techniques [27]. In short, the M_w of [PEG-PBLG-PBLA] copolymer is found to be 10,331 g/mol and the nearest step peak is 6508 g/mol. From, these two peaks, we have calculated the number of aspartic acid groups attached to it. Given that the M_w of NCA Asp is 223 g/mol, the study provides that new 18 units of aspartate are attached as a third block of polymer to the final polymer. The band at 10331 g/mol is observed which confirms the successful synthesis of [PEG-*b*-$PBLG_5$-*b*-$PBLA_{18}$] nanomicelles with an additional attachment of 18 -CH_2- units (see NMR data for the correlation, Figure 2). This study is promising for the M_w elucidation of prepared [PEG-PBLG-PBLA] copolymer.

The dynamic light scattering (DLS) technique is an intensity-based cumulative analysis performed to know the hydrodynamic radius of the polymer in an aqueous medium that includes the core plus any molecule attached or adsorbed on the surface. This study also provides strong evidence about the micelle formation of the prepared polymer. Unlike HRTEM is a number-based experiment, DLS being an intensity-weighted or volume-based experiment, provides a strong proof for the formation of micelles of [PEG-*b*-PBLG-*b*-PBLA]. As our main objective is to use this polymer for biomedical applications, therefore DLS is more appropriate. Figure S3 represents the hydrodynamic radius ranges from 70 to 400 nm (Figure S3a) and 20–250 nm (Figure S3b), respectively for [PEG-*b*-PBLG] and [PEG-*b*-PBLG-*b*-PBLA]. The newly formed [PEG-*b*-PBLG-*b*-PBLA] polymer particles lead to the self-assembly activity in the solvent medium at all ranges of pH from 4 to 10 and room temperature (RT). From this study, it is evident that the [PEG-*b*-PBLG-*b*-PBLA] polymer solution

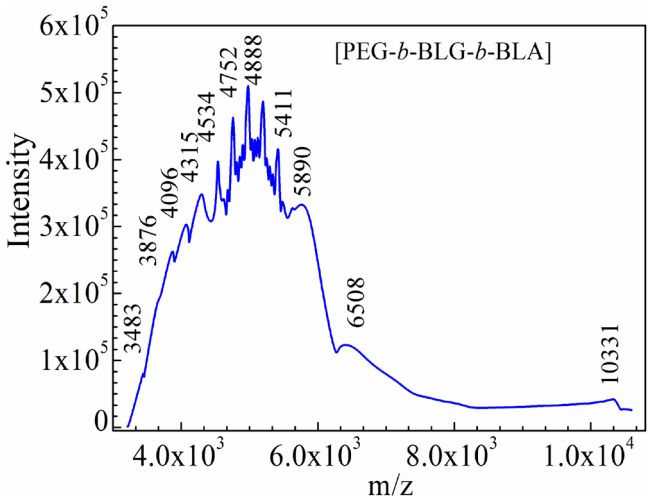

FIGURE 3 | MALDI-TOF spectrum for [PEG-*b*-BLG-*b*-BLA] triblock copolymer. [Color figure can be viewed at wileyonlinelibrary.com]

in an aqueous medium is showing a bigger size as compared to TEM in its dried state due to hydrodynamic radii and coagulation of micelles [5]. This study also represents that there is more aggregation in [PEG-*b*-PBLG] compared to [PEG-*b*-PBLG-*b*-PBLA] as we can clearly distinguish that diblock polymer is bigger than triblock copolymer. The reduction of micellar size and enhanced self-assembly activity in [PEG-*b*-PBLG-*b*-PBLA] polymer is mainly occurred due to the intermolecular H-bonding caused by the -COOH of aspartic acid and glutamic acid in the polymer. This helps the polymer to be in the micellar size range, that is, <100 nm. This helps us to understand the formation of polymer in the aqueous medium coining as nanomicelles. The shrinkage of size in [PEG-PBLG-PBLA] copolymer also proves its self-assembly nature better than the [PEG-PBLG] copolymer. The self-assembly improvement in a polymer micelle could be an efficient parameter for pharmaceutical usage of the material [17].

The HRTEM micrographs provide very interesting morphological information about the designed polymer. Figure 4a–c provides information about the spherical dot-like morphology for [PEG-*b*-PBLG] copolymer with different magnifications. The dots are seen to be evenly assembled and distributed by the amphiphilic groups in the solvent medium [28, 29]. Figure 4d–f shows the morphological evidence of [PEG-*b*-PBLG-*b*-PBLA] nanomicelles. The micrograph study suggests that all these triblock nanomicelles are less spherical with a very narrow size distribution. The shapes of [PEG-*b*-PBLG-*b*-PBLA] nanomicelles are more distorted than [PEG-*b*-PBLG] copolymer and are mainly attributed to more number of blocks present in the micelles. This mainly causes the improvement of hydrophobic-hydrophilic interaction and self-assembled attitude in the [PEG-*b*-PBLG-*b*-PBLA] nanomicelles. The average sizes of [PEG-*b*-PBLG] and [PEG-*b*-PBLG-*b*-PBLA] copolymers are found to be 22 nm and 13 nm in diameter, respectively (see Figure 4g,h). The reduction of micellar size and enhanced self-assembly properties in [PEG-*b*-PBLG-*b*-PBLA] copolymer is observed mainly due to the intermolecular H-bonding caused by the -COOH of aspartic acid and glutamic acid in the polymer chains. Another reason for lesser-sized radii of triblock copolymer micelles is due to hydrophobic part —O— ether groups being removed with hydrogenolysis. The variation of morphology for [PEG-*b*-PBLG-*b*-PBLA] copolymer is observed due to the change in the sample preparation method and parameters using deionized H_2O under ultra-sonication for a few minutes. There may be chances of electrostatic forces of attractions caused by the solvent on the surface of the polymer attracting positive and negative charged ions like -COO^- and -NH_3^+ groups leading to the formation of a fibril structure [21, 30, 31]. The prepared small-sized nanomicelles could be a very good agent for controlled drug delivery depending upon their interesting morphology.

Earlier it has been reported that block-co-polymers are mostly semicrystalline in nature [25]. The primary focus of the study is to determine the crystalline behavior of the synthesized triblock polymer. From XRD (Figure 5a), it shows that [PEG-*b*-PBLG] and [PEG-*b*-PBLG-*b*-PBLA] copolymers synthesized in this work are semicrystalline. From XRD, the diffraction peaks appear at $2\theta = 19.3°$, 23.4°, 26.7°, 27.9°, 31.6°, 36.7°, 39.9°, 43.2°, 45.4°, 48.7°, and 53.5°, respectively for the presence of smaller domain of the crystalline region of the tri-block copolymer matrix. However, the pattern has been shifted towards a low angle due to the formation of a new crystal plane with the chances

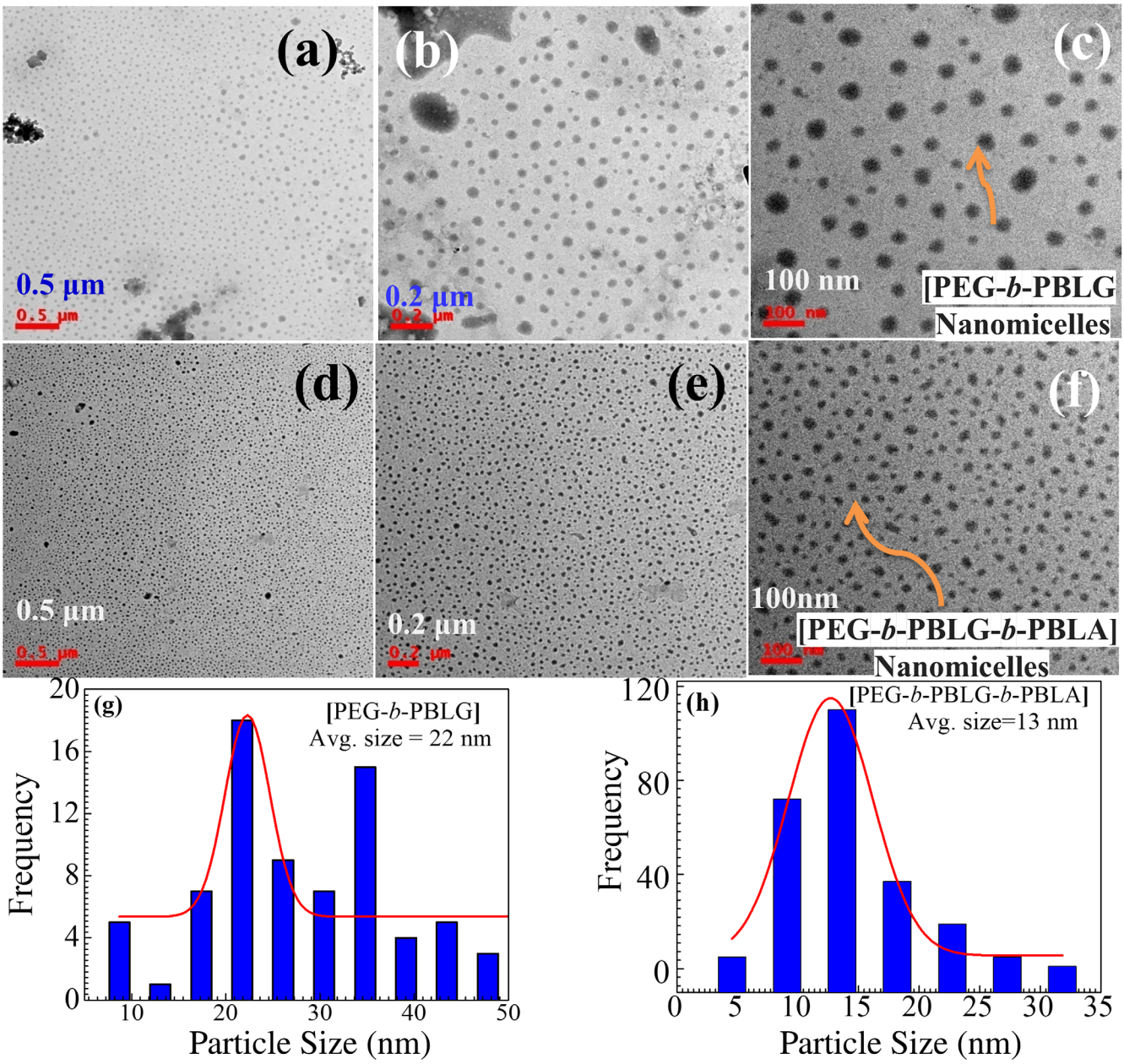

FIGURE 4 | (a–c) HRTEM micrographs of [PEG-*b*-PBLG] copolymer from lower to higher magnification. (d–f) Distorted spherical shape of [PEG-*b*-PBLG-*b*-PBLA] copolymer. (g) and (h) Histogram for the particle size distribution of [PEG-*b*-PBLG] and [PEG-*b*-PBLG-*b*-PBLA] copolymers, respectively. [Color figure can be viewed at wileyonlinelibrary.com]

of a newly formed d-spacing values [11]. The d-spacing values are observed to be 0.10, 0.13, 0.16, 0.18, 0.24, 0.26, 0.28, 0.30, 0.32, and 0.36 nm with the crystallite size ranges from 4.95 to 16.12 nm. The intensity of the XRD peaks for di-block copolymer [PEG-*b*-PBLG] is more compared to the triblock copolymer [PEG-*b*-PBLG-*b*-PBLA]. The reason for the less crystalline domain of synthesized triblock copolymer is due to a large number bulky side groups present in the backbone that hindering the triblock chain movement and folding. Other important factors such as H-bonding interaction and the orderly arrangement also can cause decrement in the crystallinity of triblock copolymer. Another evidence of crystallinity decrement can be due to the presence of intramolecular H-bonding in [PEG-PBLG-PBLA] copolymer. ^{1}HNMR study suggests that the loss of -CH_2-CH_2- groups of MeO-PEG-NH_2 block of [PEG-*b*-PBLG] diblock copolymer, whereas no such loss was observed in case of [PEG-PBLG-PBLA] triblock copolymer. This retention of -CH_2-CH_2- groups of PEG block in the [PEG-PBLG-PBLA] copolymer can be attributed to the intra-molecular hydrogen bondings between -COOH group of BLG and BLA block. This phenomenon causes the unavailability of acidic proton for the degradation of PEG-based CH_2-CH_2 group in [PEG-PBLG-PBLA] copolymer. Therefore, the addition of the NCA-BLA block to the di-block copolymer results in a decrease in the crystallinity by minimizing the loss of -CH_2_CH_2- groups in [PEG-PBLG-PBLA] copolymer. Less crystalline triblock copolymer [PEG-*b*-PBLG-*b*-PBLA] is more useful in biomedical applications as it can be degraded easily compared to di-block copolymers [32]. For more detail information about the crystalline nature and d-spacing values of polymers are shown in Table S1.

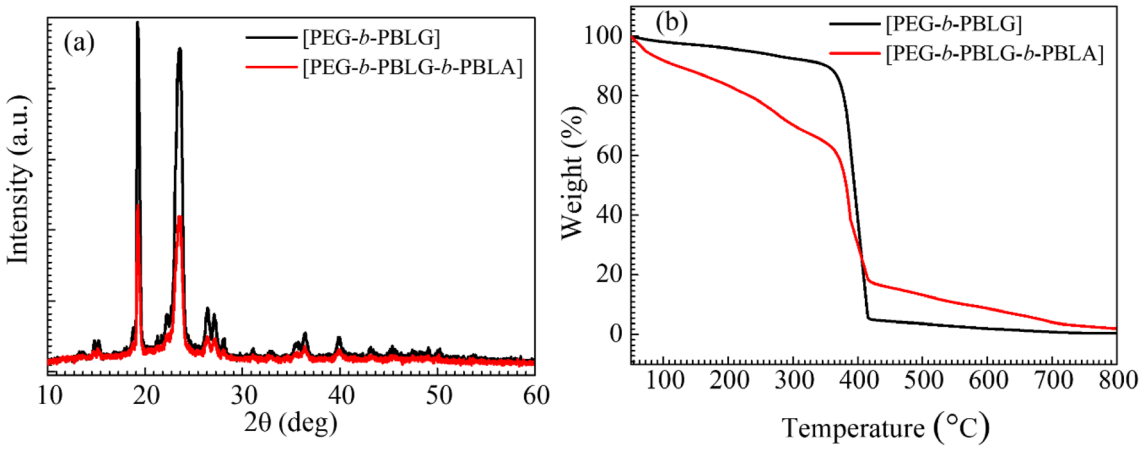

FIGURE 5 | (a) and (b) Represent XRD patterns and TGA thermograms of [PEG-*b*-PBLG] and [PEG-*b*-PBLG-*b*-PBLA] copolymers, respectively. [Color figure can be viewed at wileyonlinelibrary.com]

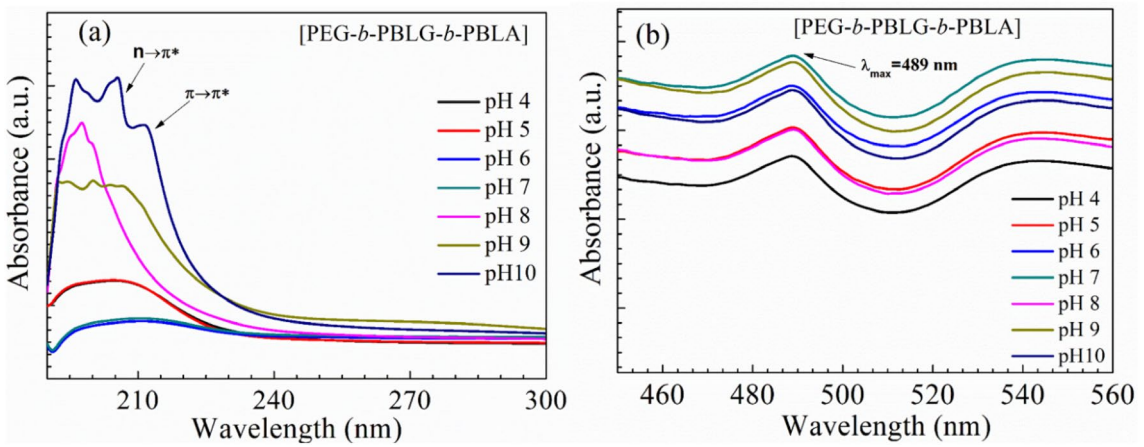

FIGURE 6 | (a) and (b) represent the UV–Vis spectra for [PEG-*b*-PBLG-*b*-PBLA] nanomicelles at the range of 190–300 nm and 450–550 nm, respectively. [Color figure can be viewed at wileyonlinelibrary.com]

Thermal stabilities of the different block copolymers were studied through TGA (Figure 5b) and found that the [PEG-*b*-PBLG-*b*-PBLA] triblock copolymer is more stable compared to the di-block copolymer [PEG-*b*-PBLG]. Being a less crystalline matter compared to diblock copolymer, [PEG-*b*-PBLG-*b*-PBLA] shows less stable before 400°C due to the higher disorders in the arrangement leading to the relaxation of chain movement in the polymer. Slow degradation of [PEG-*b*-PBLG-*b*-PBLA] polymer occurs only at a higher temperature (after 400°C) compared to the di-block copolymers. For [PEG-*b*-PBLG-*b*-PBLA] copolymer, a continuous weight loss is observed before 200°C. However, for [PEG-*b*-PBLG-*b*-PBLA] polymer, the weight loss before 400°C is occurred mostly due to the degradation of weight of volatile low molecular weight polymer chains and may be due to the degradation of a few side groups present along with more organic groups attached to the backbone of polymer. However, after 400°C the [PEG-*b*-PBLG-*b*-PBLA] shows comparatively less weight loss till 800°C due to the covalent bonding associated with the polymer chains. There are a very few biocompatible polymers reported with the degradation of polymers after 400°C. Thus, the synthesized tri-block copolymer [PEG-*b*-PBLG-*b*-PBLA] is thermally more stable compared to the di-block copolymer [PEG-*b*-PBLG] after 400°C–800°C [33]. However, thermal stability is very much crucial for [PEG-*b*-PBLG-*b*-PBLA] copolymer for its use in various biomedical applications [3, 4].

The presence of labile electrons and the functional groups present in the polymer structure were characterized through UV–Vis spectroscopy. The broad absorption band that appeared in UV–Vis spectra indicates the presence of chromophoric groups such as -(C=O)-NH_2 and (-C=O) (at 220 nm and 206 nm, respectively) (See Figure 6). These bands appeared due to the free electron transfer from nonbonding orbitals to π antibonding orbital causing $n \rightarrow \pi^*$ and $\pi \rightarrow \pi^*$ transitions for carbonyl and amide bonding. We have scanned the UV–Vis absorption of [PEG-*b*-PBLG-*b*-PBLA] nanomicelles at RT by varying pH from 4 to 10. From Figure 6, it is obvious that with decrease in pH, the intensity of absorption bands decreases as the number of active acid chromophores in the solution medium increases and leads to the broadening of the absorption bands. However, the number of active amine chromophores increases at pH 10 resulting in a sharp and intense absorption band. A very small absorption band at 489 nm appeared indicating the presence of protein (-NH_2) and —OH group [34]. Figure S4 also shows absorption due to the occurrence of a similar mechanism of the copolymer of [PEG-*b*-PBLG] with a wavelength of maximum at 195 nm caused by –COOH groups associated with them.

A laser scanning confocal experiment is performed to give concrete evidence about the formation of amino-acid-based triblock copolymeric micelles. The polymers were loaded with

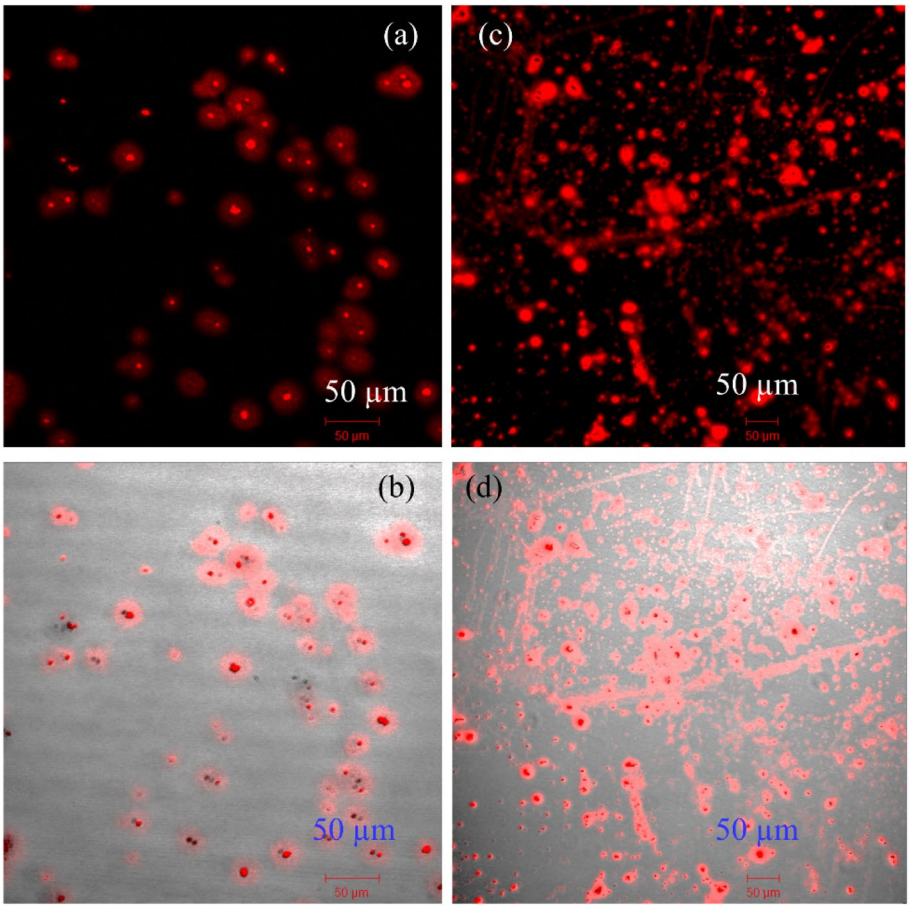

FIGURE 7 | Laser Confocal microscopy images of [PEG-*b*-PBLG] (a, b) and for [PEG-*b*-PBLG-*b*-PBLA] nanomicelles for laser and bright-field images (c, d), respectively. [Color figure can be viewed at wileyonlinelibrary.com]

Rhodamine 6G molecules along with several times washing. Figure 7a,b show the confocal microscopic images of the [PEG-*b*-PBLG]. Figure 7c,d show the confocal microscopic images for the [PEG-*b*-PBLG-*b*-PBLA]. For both the polymers, it is evident that the micelles are spherical in nature and are capable of loading small biomolecules. Rhodamine 6G molecules are loaded inside the micelles and on excitation with laser light, they emit red fluorescent light. Both the confocal microscopy and HRTEM micrographs revealed that [PEG-*b*-PBLG] and [PEG-*b*-PBLG-*b*-PBLA] micelles are spherical in nature. Hydrophilicity behavior and the amphiphilic nature of the polymers led to the formation of micelles with the reluctance of solvation property of hydrophobic groups, which caused the particle size to decrease sharply [25, 35–38]. The self-association property along with intermolecular hydrogen bonding between cationic and anionic groups of [PEG-*b*-PBLG] and [PEG-*b*-PBLG-*b*-PBLA] in a suitable solvent medium lead to the formation of micelles [39, 40].

The solubility of the [PEG-*b*-PBLG-*b*-PBLA] is checked in a various solvent medium, for example, in THF, acetone, ethanol, 1, 2-dioxane, DMSO, cyclohexane, chloroform, DMF, toluene, water, and ether. In this work, we have chosen DDI water as our solvent due to the suitability of water for biological applicability. For the sample for zeta potential (ζ) measurement, we have prepared dispersion at 0.5 mg/mL conc. at 25°C. Figure 8a,b represented the stability of colloidal dispersion of [PEG-*b*-PBLG-*b*-PBLA] and [PEG-*b*-PBLG] copolymers, respectively at different pH ranges. Results show that [PEG-*b*-PBLG-*b*-PBLA] nanomicelles have more ζ values than [PEG-*b*-PBLG] due to the presence of more functional groups [41, 42]. It is evident that with change in pH from 4 to 10, both the polymers are coagulated and responsive toward the colloidal particle formation. The ζ of [PEG-*b*-PBLG-*b*-PBLA] micelles are seen to have a maximum value of −44.6 mV at pH 10, whereas for [PEG-*b*-PBLG] micelles possess to be $\zeta = -34$ mV at pH 8. The minimum ζ value found for [PEG-*b*-PBLG-*b*-PBLA] micelles is approximately 1 mV at pH 4. Furthermore, [PEG-*b*-PBLG-*b*-PBLA] micelles exhibit two distinct peaks as shown in Figure 8a. These peaks are appeared mainly due to the presence of two different pKa values (pKa1 (acidic COOH)) and pKa2 (basic NH_2) caused by available dissociated ions in the medium and due to the distribution of particles size. The inter-ionic, as well as H-bonding interactions on the micelle's surface of [PEG-b-PBLG-b-PBLA], lead to the increase in the ζ value. This value seems to be higher in the basic medium (up to $\zeta = -45$ mV) compared to the values obtained in the acidic medium (maximum obtained $\zeta = -9$ mV). In addition to the solvent effects, OH^- groups also influence the surface activation (properties) providing H-interactions among the polymeric micellar solution. The reversal of the positive charge on the carboxylic group tends to the electronic delocalization and leads to the formation of a neutral (charge) environment. The surface charge of [PEG-b-PBLG-b-PBLA] has consisted of several –COOH groups. Upon the addition of NH_4OH solution to the medium, it was immediately converted into -COO^- which

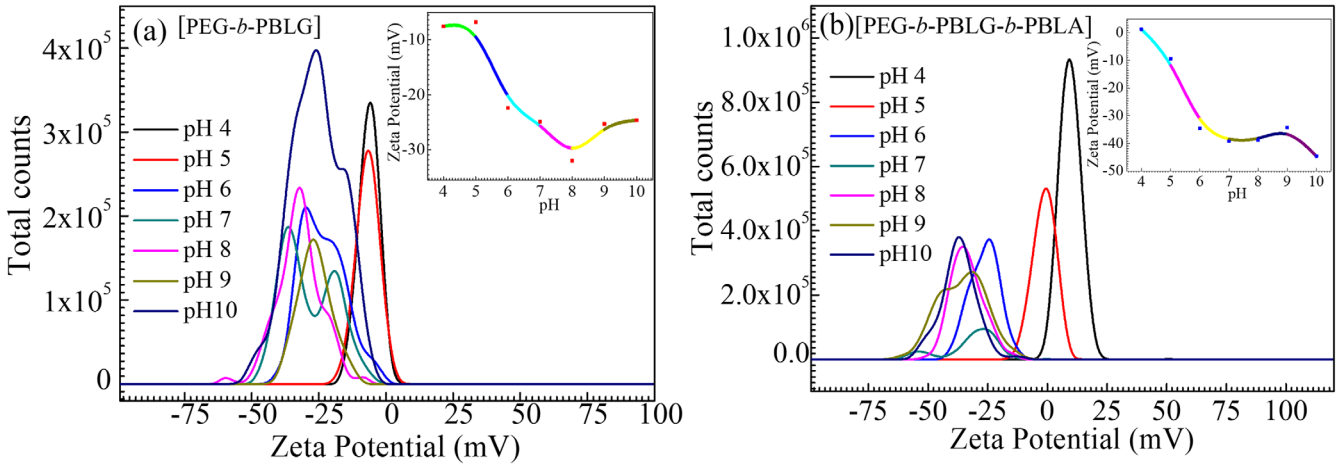

FIGURE 8 | (a) and (b) Profiles for zeta potential for [PEG-*b*-PBLG] and [PEG-*b*-PBLG-*b*-PBLA] nanomicelles, respectively at different pH (pH 4 to10) and 25°C. [Color figure can be viewed at wileyonlinelibrary.com]

repels the adjacent -COO^- groups of [PEG-*b*-PBLG-*b*-PBLA] copolymer micelles resulting in higher ζ values. However, the addition of acid (H^+) to the polymer solution, hinders the formation of cations at the surface of the micelles of block copolymers. The reason for the increase in ζ value is due to the reversibility nature of –COOH groups and the act of -COO- as counter ions in salvation [37, 43, 44]. The highest ζ value for [PEG-*b*-PBLG] micelles is obtained to be −30 mV at pH 8 which showed the highest stability. Whereas, the ζ value of the [PEG-*b*-PBLG-*b*-PBLA] solution is stable at all the pH values (6–10) at 25°C (see Table S2). The detailed ζ values for [PEG-*b*-PBLG] and [PEG-*b*-PBLG-*b*-PBLA] solutions are shown in Table S2.

3.2 | CD Analysis for Amino-Acid-Based Polymeric Proteins With Varying pH and Temperature

The nature of the secondary structure of the synthesized block copolymers was studied through the CD analysis (Figure 9). It is observed that the secondary structure of the block copolymer (concentration 0.5 mg/mL) changes with the change in pH and temperature. It can be noted that the self-assembly behavior of the block copolymers is influenced by pH, temperature, and concentration of the medium. The synthesized block copolymers are consist of the mixture of both helical and random coil configurations [45–48].

From Figure 9, it is calculated that the triblock copolymer of [PEG-*b*-PBLG-*b*-PBLA] consists of 6.0% α-helix, 49.0% antiparallel β-sheets, 3.7% parallel β-sheets, 16.6% β-Turns, and 29.2% random coils at 35°C and pH 8. Table S3 provides the detailed percentage of protein folding structure in [PEG-*b*-PBLG-*b*-PBLA] block copolymer at 35°C with pH 4–10. The antiparallel β-sheets are calculated to be up to 50% for tri-block copolymers synthesized in this work and they are exhibiting protein-like structure in pH 4 to 10. From the graph, it is evident that, the structural conformation of the [PEG-*b*-PBLG-*b*-PBLA] copolymer also has been changed with pH and temperature. The higher percentage of the anti-parallel β-sheet structure is observed due to the presence of more peptide bonds (-C=O-NH-) associated with each other through H-bonding in the solvent medium. The variation seems to be distinctly increased from 20°C to 50°C. Although the difference in the percentage of α-helix, β-sheets, and random coils are obtained at numerous temperatures and pH, however, there is no significant change in values observed compared to the values obtained at 35°C and pH 8. The synthesized block copolymers exhibit bands with low intensity at 220 and 190 nm at 35°C. The band at 220 nm is attributable to the $n \rightarrow \pi^*$ transition of the peptide bonds in the block copolymer chains. Major CD bands appeared at 208 nm (less intense) and 193 nm (maximum intensity) contributed by the parallel and perpendicular excitations of the $\pi \rightarrow \pi^*$ transition of the [PEG-*b*-PBLG-*b*-PBLA] triblock copolymer due to the higher percentage of antiparallel β-sheets in the solution. However, the CD band intensities are not acting in the same way among the three sets of reference proteins including ours (CDNN), since the nature of the spectrum of CD components depends on the reference proteins used for the deconvolution [49–51]. Figure S5 illustrates CD results for [PEG-*b*-PBLG] diblock copolymer obtained at 20°C–50°C with varying pH, exhibiting less ellipticity than [PEG-*b*-PBLG-*b*-PBLA]. The nature of folding of the chains for [PEG-*b*-PBLG] copolymers is less due to the less electrostatic interactions acting between the peptide bond which ceases its ellipticity compared to the [PEG-*b*-PBLG-*b*-PBLA] triblock polymer. From, the CD study, it is evident that the prepared [PEG-*b*-PBLG-*b*-PBLA] triblock polymer can be useful as synthetic polypeptides for biomedical applications [50].

3.3 | In Vitro Cytotoxicity Assay of the Block Copolymers

Biocompatibility of the block copolymer micelles is important for its use in therapeutic purposes. Therefore, the cell viability assay was performed following the previous methods [52] Figure 10. Previous work reported the cell viability of similar diblock copolymeric materials against non-carcinoma cell lines with a viability of ~100% [25]. Another report by Jin et al. discussed the viability of the synthesized diblock copolymer micelles [PEG-*b*-PBLG] against HeLa cells, showing decreased in viability with increased in the concentrations up to 50 μg/mL, proving the polymeric micelles as less cytotoxic performance and good biocompatibility [21]. In this work, c the cancer cell inhibition efficiency of the synthesized block copolymers have been studied through the MTT assay by varying the concentrations. In

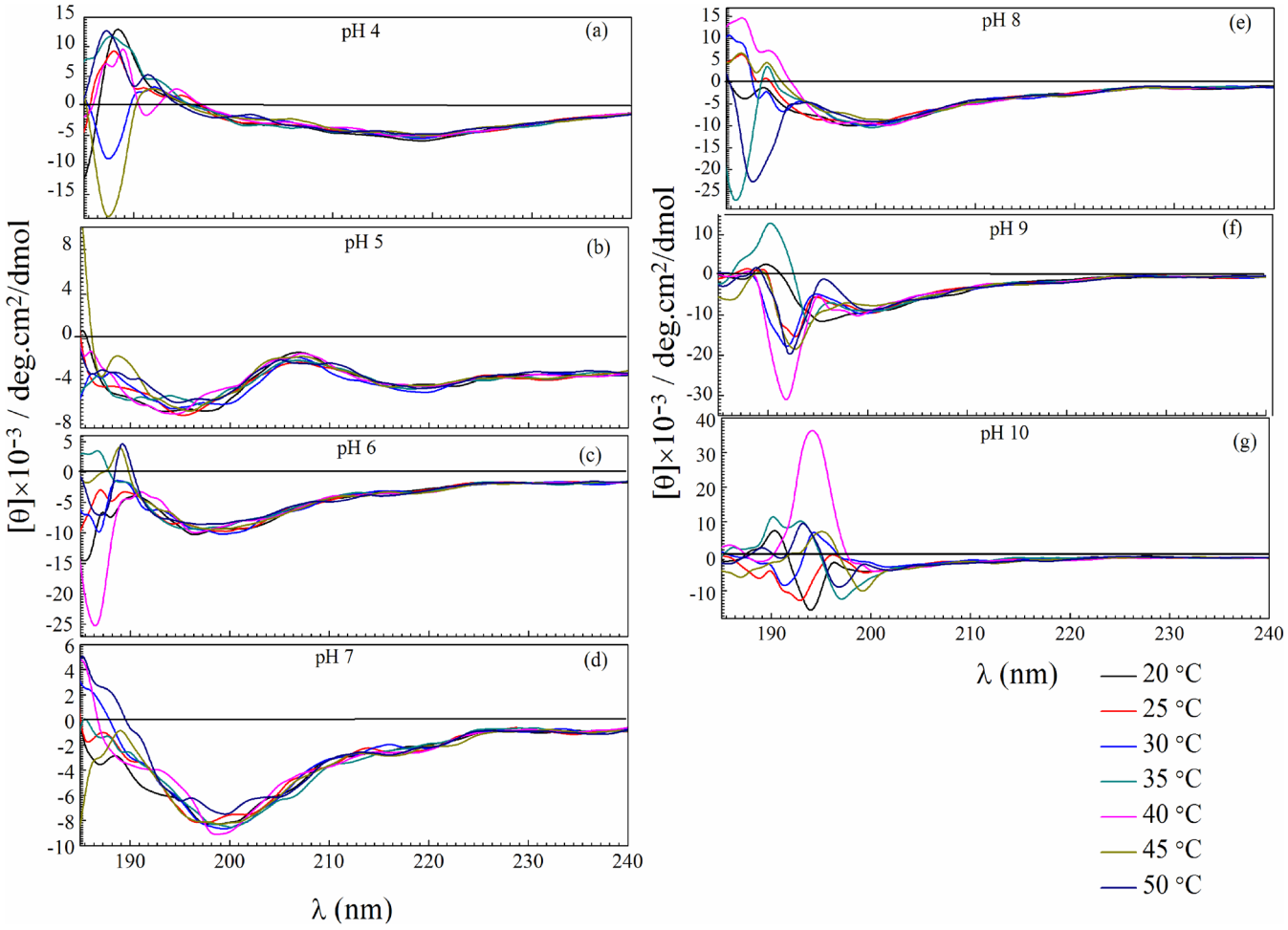

FIGURE 9 | Illustrates the CD results for [PEG-*b*-PBLG-*b*-PBLA] nanomicelles at 20°C–50°C with different pH: (a) pH 4, (b) pH 5, (c) pH 6, (d) pH 7, (e) pH 8, (f) pH 9, and (g) pH 10, respectively. [Color figure can be viewed at wileyonlinelibrary.com]

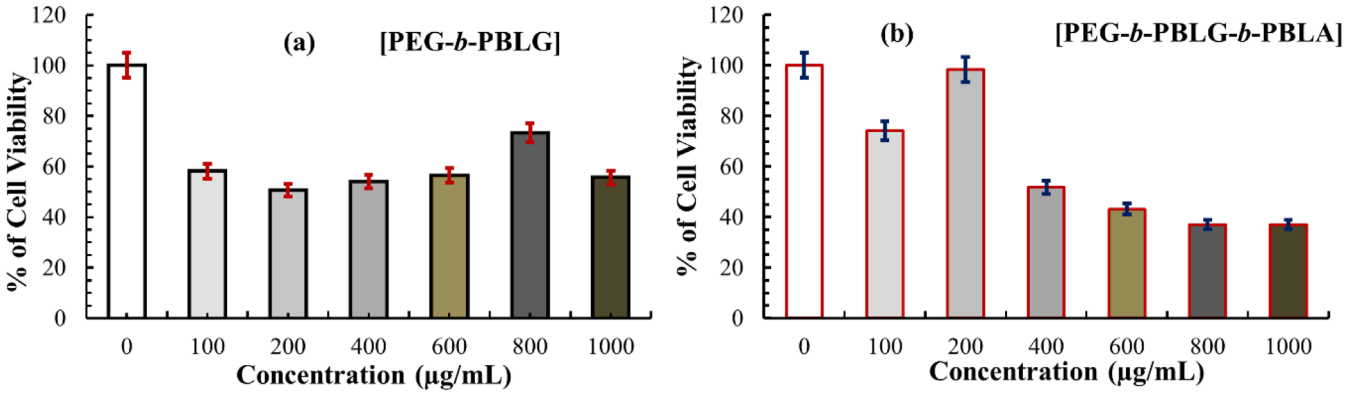

FIGURE 10 | Cell viability results for [PEG-*b*-PBLG] and [PEG-*b*-PBLG-*b*-PBLA] nanomicelles, respectively tested against MDA-MB-231 cell lines. [Color figure can be viewed at wileyonlinelibrary.com]

brief, [PEG-*b*-PBLG] and [PEG-*b*-PBLG-*b*-PBLA] samples were dispersed in DMEM medium with mild sonication and treated with MDA-MB-231 cell lines (human carcinoma cells), taking 5×10^3 cells/well for 24 h incubation in 96-well plates with different concentrations of polymers.

The viability of cells was assessed by adding 10 µL of MTT solution (stock solution 5 mg mL^{-1}) per well and incubating at 37°C for 3 h. The medium was discarded, and the formazan blue, which formed in the cells, was dissolved in 100 µL of DMSO. The intensity of color formation was measured at 570 nm (background 665 nm). The percentage of cell viability was calculated and compared with the control values (without the test compound). Cell viability assay was performed for both the sets of polymers in DMEM medium treated against MDA-MB-231 cells for 24 h resulting in pure cell viable up to 200 µg/mL of concentration for [PEG-*b*-PBLG-*b*-PBLA] block copolymers, however caused a significant decrease in viability

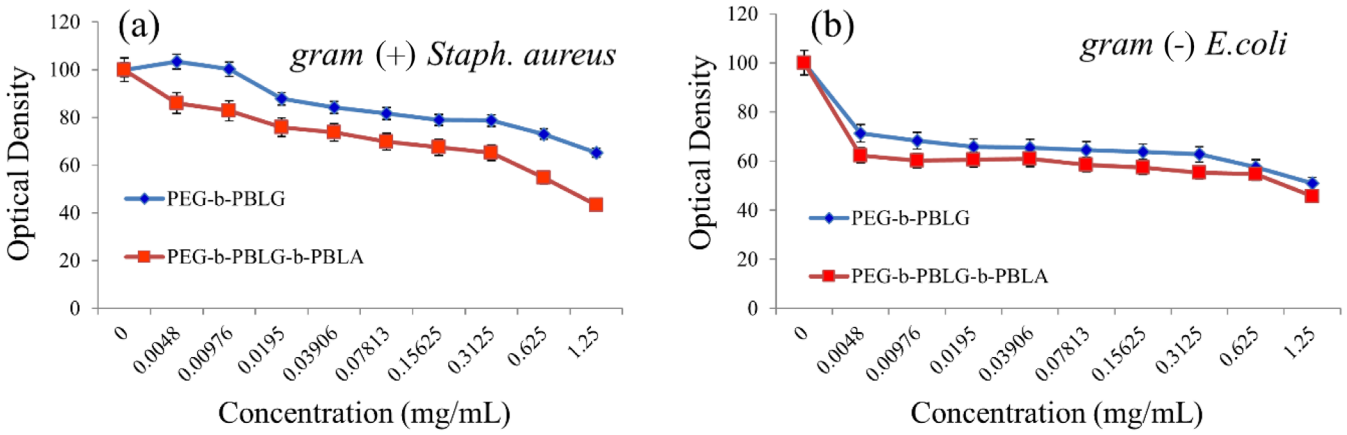

FIGURE 11 | (a) and (b) in vitro antimicrobial activity results of [PEG-*b*-PBLG] and [PEG-*b*-PBLG-*b*-PBLA] nanomicelles for Gram (+) *S. aureus* and Gram (–) *E. coli*, *respectively.* [Color figure can be viewed at wileyonlinelibrary.com]

with increase in the concentrations. It is observed that the percentage of cell viability gradually decreases from 95% to lower values with an increase in the concentrations and significantly changes after 200 μg/mL. Whereas, even at a minimum concentration of [PEG-*b*-PBLG], it exhibits toxicity. As an example, at a concentration of 100 μg/mL the cell viability is obtained to be 50%. In short, cancer cell growth inhibition is observed to be 25.22%–63.85% after treatment in [PEG-*b*-PBLG-*b*-PBLA], whereas 41.16%–45.06% in [PEG-*b*-PBLG] at the concentration of 100 and 1000 μg/mL, respectively. Figure S6a,b represent the IC_{50} values recorded in the graph for [PEG-*b*-PBLG-*b*-PBLA] and [PEG-b-PBLG] nanomicelles. The IC_{50} is an important specification to measure the cell death of synthesized polymer without any external drug or agent. The IC_{50} values for [PEG-b-PBLG] and [PEG-*b*-PBLG-*b*-PBLA] polymers are calculated to be 560.340 ± 34.107 μg/mL and 750.468 ± 47.312 μg/mL, respectively. Therefore, the [PEG-*b*-PBLG-*b*-PBLA] nanomicelles exhibit significant toxicity effects on the cancer cells without using any conventional chemotherapy drug use for cancer therapy. Further to check the medical applications of these block co-polymers, they are used to find out the effect on the bacteria strains and discussed in the subsequent section.

3.4 | In Vitro Antibacterial Activity

Previous works reported that the polymeric materials associated with the quaternary ammonium salts can be used in antibacterial activities [53, 54]. The presence of quaternary ammonium salts, it has increased the antimicrobial activity of the prepared material which attracted us to perform the further study against bacterial strains. Figure 11a shows the effective killing efficiency of Gram (+) *S. aureus* at 0.156, 0.3125, 0.625, and 1.25 mg/mL with the lowest minimum inhibitory concentration (MIC) and OD of 60%, 57%, 50%, and 40%, respectively [55]. The low OD value for triblock copolymers [PEG-*b*-PBLG-*b*-PBLA] against positive strain is very interesting compared to the results obtained for [PEG-*b*-$PBLG_5$] micelles. The [PEG-*b*-PBLG-*b*-PBLA] always exhibited better antibacterial effects than that of [PEG-*b*-PBLG] micelles. This result is obtained may be due to the presence of a more numbers of quaternary ammonium salts (amine-functionalized groups) in the medium which ceases the bacterial survival effectively.

Figure 11b also shows an excellent low OD for synthesized [PEG-*b*-PBLG-*b*-PBLA] polymeric micelles than [PEG-*b*-PBLG] micelles against the Gram (–) *E. coli*, indicating the effective killing of bacterial cells at a concentration of 1.25 mg/mL for both the strains. With the decrease of polymeric micelle's concentrations up to the lowest value of 0.0048 mg/mL, the killing efficiency of [PEG-*b*-PBLG-*b*-PBLA] polymeric nanomicelles is higher in gram (–) strain of *E. coli* compared to the [PEG-*b*-PBLG] copolymer. Further, [PEG-*b*-PBLG-*b*-PBLA] shows relatively a very good antibacterial effect against gram (–) *E. coli* at a very minimum dilution of 0.0048 mg mL^{-1} than gram (+) *S. aureus*. Additionally, at 0.07813 mg mL^{-1} of [PEG-*b*-PBLG-*b*-PBLA] polymer micelles, the bacterial cells show a very low difference in percentage of survival than [PEG-*b*-PBLG] polymer, indicating better use for inhibition of the growth of microbial at the negative strain. The lower OD values are observed for both types of strains with [PEG-*b*-PBLG-*b*-PBLA] micelles indicating the increased disintegration of dead cells. The OD values for both the micelles are tabulated in Table S4. It followed the probable reactive oxygen species (ROS) mechanism to destroy the bacteria. As the polymeric micelles interact and enter through the cell wall of the bacterium and they lead to the formation of reactive free radicals due to the presence of ions in the solution medium causing the oxidation with the rupture of DNAs, lipids, and folding of proteins by single electron mechanism process. The entire process is shown in Scheme 2 which follows the ROS mechanism pathway to damage the bacterial DNAs. The synthesized polymeric micelles in nanometer range could be a very good option for drug delivery applications, and antiseptic properties and antitumor activities fulfill outstanding biomedical applications [56, 57]. Thus, it can be concluded that these two polymeric nano micelles are capable of antimicrobial activity and can be used for other biomedical applications.

4 | Conclusions

To put all the aspects succinctly, biocompatible, and ecologically viable approach is adopted for the design of

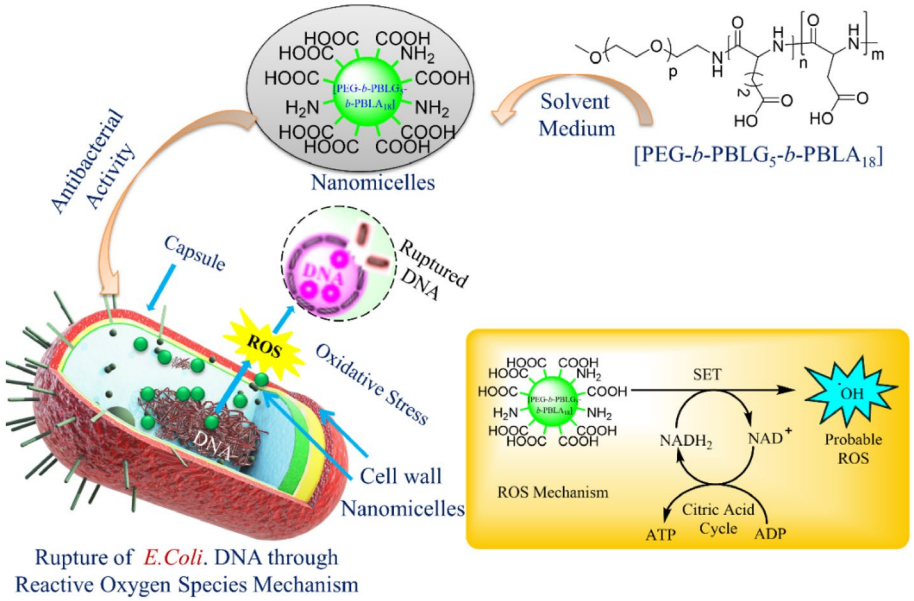

SCHEME 2 | Generation of reactive oxygen species (ROS) and mechanism for the killing of bacteria by the nanomicelles. [Color figure can be viewed at wileyonlinelibrary.com]

[PEG-*b*-PBLG-*b*-PBLA] polymeric micellies. It is revealed that the controlled surface morphology and electrostatic interactions played a prime role in the formation of micelles. Improved colloidal stability of the prepared polymeric micellies indicated by the high zeta potential owing to the chemical interaction between the functional groups present in the polymeric chains. The CD results for [PEG-*b*-PBLG-*b*-PBLA] polymer with a high percentage of anti-parallel β-sheets revealed its effective use in therapeutic applications. Due to host-guest inclusion complex formation activity, this polymer can form complexes with various proteins, peptides, metals, and other biocompatible materials which further can be used as a drug delivery medium. The cell viability results for [PEG-*b*-PBLG-*b*-PBLA] polymer against MDA-MB-231 human breast carcinoma are found to be effective for the treatment of cancer with IC_{50} values of 750.468 ± 47.312 μg/mL. These results also provide a strong insight that at lower concentrations such as 200 μg/mL, the micelles can be used as anticancer agents. Further, the antibacterial study for [PEG-*b*-PBLG-*b*-PBLA] copolymers revealed that, it further could be an effective component for killing gram (−) *E. Coli* and gram (+) *S. aureus*. Thus, it can be concluded that the designed polymeric micellies could be an effective component for anti-cancer as well as anti-bacterial applications.

Author Contributions

Pradip Paik: conceptualization (lead), formal analysis (lead), funding acquisition (lead), investigation (lead), methodology (lead), project administration (lead), supervision (lead), writing – original draft (lead), writing – review and editing (lead). **Debasrita Bharatiya:** formal analysis (supporting), methodology (supporting), writing – original draft (supporting), writing – review and editing (supporting). **Biswajit Parhi:** formal analysis (supporting), methodology (supporting), writing – review and editing (supporting). **Khumukcham Saratchandra Singh:** formal analysis (supporting), methodology (supporting), writing – review and editing (supporting). **Bramanandam Manavathi:** formal analysis (supporting), supervision (supporting), writing – review and editing (supporting).

Acknowledgments

Authors acknowledge the research support grants awarded by DST-Nanomission, India (Ref: SR/NM/NS-1005/2015), Science and Engineering Research Board, India (Ref: EEQ/2016/000040 and CRG/2023/005576), India, I-DAPT foundation (Ref. I-DAPT/IT (BHU)/2023-24/ Project Sanction/47), STARS-IISc. Bangalore (Ref. MoE-STARS/STARS-2/2023-0318), ICMR (Ref. IIPR-2023-4724/F1), and Seed grants (OH-35) supported by Indian Institute of Technology (BHU), to Prof. Paik. Debasrita Bharatiya acknowledges UGC New Delhi, India for providing fellowship and Rutuparna Jena for her assistance in performing the experiments.

Conflicts of Interest

The authors declare no conflicts of interest.

Data Availability Statement

The data that support the findings of this study are available from the corresponding author upon reasonable request.

References

1. S. Lv, M. Li, Z. Tang, et al., "Doxorubicin-Loaded Amphiphilic Polypeptide-Based Nanoparticles as an Efficient Drug Delivery System for Cancer Therapy," *Acta Biomaterialia* 9 (2013): 9330–9342.

2. G. Zhu, F. Wang, K. Xu, S. Dong, and Y. Liu, "Properties Study of Poly(l-Lactic Acid)/poly(γ-Benzyl l-Glutamate)-graft-Poly(Ethylene Glycol) Blend Film," *Research on Chemical Intermediates* 41 (2015): 1097–1106.

3. P. K. Sethy, P. Mohapatra, S. Patra, D. Bharatiya, and S. K. Swain, "Antimicrobial and Barrier Properties of Polyacrylic Acid/GO Hybrid Nanocomposites for Packaging Application," *Nano-Structures & Nano-Objects* 26 (2021): 100747.

4. B. Parhi, D. Bharatiya, and S. K. Swain, "Application of Quercetin Flavonoid Based Hybrid Nanocomposites: A Review," *Saudi Pharmaceutical Journal* 28 (2020): 1719–1732.

5. S. Perumal, R. Atchudan, and W. Lee, "A Review of Polymeric Micelles and Their Applications," *Polymers (Basel)* 14 (2022): 2510.

6. J. M. Widin, A. K. Schmitt, A. L. Schmitt, K. Im, and M. K. Mahanthappa, "Unexpected Consequences of Block Polydispersity on the Self-Assembly of ABA Triblock Copolymers," *Journal of the American Chemical Society* 134 (2012): 3834–3844.

7. S. W. Li, M. F. Hsieh, T. Hong, et al., "Block Copolymer-Stabilized Metal–Organic Framework Hybrids Loading Pd Nanoparticles Enable Tumor Remission Through Near-Infrared Photothermal Therapy," *Advanced NanoBiomed Research* 4 (2024): 2470011.

8. M. Holeček, "Aspartic Acid in Health and Disease," *Nutrients* 15 (2023): 4023.

9. F. F. V. dos Santos, S. Habelitz, F. D. Nascimento, V. E. Arana-Chavez, and R. R. Braga, "Poly(Aspartic Acid) Promotes Odontoblast-Like Cell Differentiation in Rat Molars With Exposed Pulp," *Journal of Functional Biomaterials* 14 (2023): 537.

10. J. Yan, P. F. Marina, and A. Blencowe, "A Facile Strategy for the High Yielding, Quantitative Conversion of Polyglycol End-Groups to Amines," *Polymers (Basel)* 13 (2021): 1403.

11. J. Sun, Z. Wang, C. Zhu, et al., "Hierarchical Supramolecular Assembly of a Single Peptoid Polymer Into a Planar Nanobrush With Two Distinct Molecular Packing Motifs," *Proceedings of the National Academy of Sciences of the United States of America* 117 (2020): 31639–31647.

12. B. Parhi, D. Bharatiya, and S. K. Swain, "Effect of Polycaprolactone on Physicochemical, Biological, and Mechanical Properties of Polyethylene Oxide and Polyaminoacids Nanoblock copolymer," *Journal of Applied Polymer Science* 139 (2022): 52116.

13. D. Bharatiya, S. Patra, B. Parhi, and S. K. Swain, "A Materials Science Approach Towards Bioinspired Polymeric Nanocomposites: A Comprehensive Review," *International Journal of Polymeric Materials and Polymeric Biomaterials* 72 (2021): 119.

14. H. Zhu, Y. Liu, D. Gu, Z. Rao, Y. Li, and J. Hao, "Dual Thermoresponsive mPEG-b-Poly(O-Benzyl-l-Threonine Acid) Hydrogel Based on β-Sheet Nano-Structural Disassembly and PEG Dehydration," *Polymer (Guildf)* 226 (2021): 123841.

15. H. Zhu, D. Gu, Z. Rao, Y. Li, Y. Liu, and J. Hao, "Design of Gel-To-Sol UCST Transition Peptides by Controlling Polypeptide β-Sheet Nanostructures," *Polymer Journal* 53 (2021): 943–949.

16. X. Wang, S. Yan, L. Song, et al., "Temperature-Responsive Hierarchical Polymer Brushes Switching From Bactericidal to Cell Repellency," *American Chemical Society Applied Materials & Interfaces* 9 (2017): 40930–40939.

17. T. Miyazaki, K. Igarashi, Y. Matsumoto, and H. Cabral, "One-Pot Synthesis of PEG–Poly(Amino Acid) Block Copolymers Assembling Polymeric Micelles With PEG-Detachable Functionality," *American Chemical Society Biomaterials Science & Engineering* 5 (2019): 5727–5733.

18. H. Xu, P. Yang, H. Ma, et al., "Amphiphilic Block Copolymers-Based Mixed Micelles for Noninvasive Drug Delivery," *Drug Delivery* 23 (2016): 3063–3071.

19. A. Basu, K. R. Kunduru, J. Katzhendler, and A. J. Domb, "Poly(α-Hydroxy Acid)s and Poly(α-Hydroxy Acid-Co-α-Amino Acid)s Derived From Amino Acid," *Advanced Drug Delivery Reviews* 107 (2016): 82–96.

20. P. Paik, A. Gedanken, and Y. Mastai, "Enantioselective Separation Using Chiral Mesoporous Spherical Silica Prepared by Templating of Chiral Block Copolymers," *American Chemical Society Applied Materials & Interfaces* 1 (2009): 1834–1842.

21. J. Jin, B. Sui, J. Gou, et al., "PSMA Ligand Conjugated PCL-PEG Polymeric Micelles Targeted to Prostate Cancer Cells," *PLoS One* 9 (2014): e112200.

22. J. De Meutter and E. Goormaghtigh, "Amino Acid Side Chain Contribution to Protein FTIR Spectra: Impact on Secondary Structure Evaluation," *European Biophysics Journal* 50 (2021): 641–651.

23. A. K. Yamala, V. Nadella, Y. Mastai, H. Prakash, and P. Paik, "Poly-N-Acryloyl-(l-Phenylalanine Methyl Ester) Hollow Core Nanocapsules Facilitate Sustained Delivery of Immunomodulatory Drugs and Exhibit Adjuvant Properties," *Nanoscale* 9 (2017): 14006–14014.

24. K. N. Sill, B. Sullivan, A. Carie, and J. Edward Semple, "Synthesis and Characterization of Micelle-Forming PEG-Poly(Amino Acid) Copolymers With Iron-Hydroxamate Cross-Linkable Blocks for Encapsulation and Release of Hydrophobic Drugs," *Biomacromolecules* 18 (2017): 1874–1884.

25. C. Amgoth, G. Dharmapuri, A. M. Kalle, and P. Paik, "Nanoporous Capsules of Block Co-Polymers of [(MeO-PEG-NH)-b-(L-GluA)]-PCL for the Controlled Release of Anticancer Drugs for Therapeutic Applications," *Nanotechnology* 27 (2016): 125101.

26. M. Deng, R. Wang, G. Rong, et al., "Synthesis of a Novel Structural Triblock Copolymer of Poly(γ-Benzyl-l-Glutamic Acid)-b-Poly(Ethylene Oxide)-b-Poly(ε-Caprolactone)," *Biomaterials* 25 (2004): 3553–3558.

27. L. Y. Wang, S. G. Wang, and J. Z. Bei, "Synthesis and Characterization of Macroinitiator-Amino Terminated PEG and Poly(γ-Benzyl-L-Glutamate)-PEO-Poly(γ-Benzyl-L-Glutamate) Triblock Copolymer," *Polymers for Advanced Technologies* 15 (2004): 617–621.

28. X. J. Loh, Z. X. Zhang, Y. L. Wu, T. S. Lee, and J. Li, "Synthesis of Novel Biodegradable Thermoresponsive Triblock Copolymers Based on Poly[(R)-3-Hydroxybutyrate] and Poly(N-Isopropylacrylamide) and Their Formation of Thermoresponsive Micelles," *Macromolecules* 42 (2009): 194–202.

29. M. R. Libera and R. F. Egerton, "Advances in the Transmission Electron Microscopy of Polymers," *Polymer Reviews* 50 (2010): 321–339.

30. W. Zhao, D. Chen, Y. Hu, G. M. Grason, and T. P. Russell, "ABC Triblock Copolymer Vesicles With Mesh-Like Morphology," *American Chemical Society Nano* 5 (2011): 486–492.

31. S. Xu, C. Zhang, L. Li, and S. Zheng, "Polystyrene-Block-Polyethylene-Block-Polystyrene Triblock Copolymers: Synthesis and Crystallization-Driven Self-Assembly Behavior," *Polymer (Guildf)* 128 (2017): 1–11.

32. R. Pantani and A. Sorrentino, "Influence of Crystallinity on the Biodegradation Rate of Injection-Moulded Poly(Lactic Acid) Samples in Controlled Composting Conditions," *Polymer Degradation and Stability* 98 (2013): 1089–1096.

33. D. M. Nascimento, J. S. Almeida, A. F. Dias, et al., "A Novel Green Approach for the Preparation of Cellulose Nanowhiskers From White Coir," *Carbohydrate Polymers* 110 (2014): 456–463.

34. J. Sundaram, B. Park, A. Hinton, K. C. Lawrence, and Y. Kwon, "Detection and Differentiation of Salmonella Serotypes Using Surface Enhanced Raman Scattering (SERS) Technique," *Journal of Food Measurement and Characterization* 7 (2013): 1–12.

35. B. A. Chalmers, C. Magee, D. L. Cheung, P. B. Zetterlund, and F. Aldabbagh, "CO_2-Responsive Polyacrylamide Copolymer Vesicles With Acid-Sensitive Morpholine Moieties and Large Hydrophobic RAFT End-Group," *European Polymer Journal* 97 (2017): 129–137.

36. M. G. Carneiro-Da-Cunha, M. A. Cerqueira, B. W. S. Souza, J. A. Teixeira, and A. A. Vicente, "Influence of Concentration, Ionic Strength and pH on Zeta Potential and Mean Hydrodynamic Diameter of Edible Polysaccharide Solutions Envisaged for Multinanolayered Films Production," *Carbohydrate Polymers* 85 (2011): 522–528.

37. L. Zhu, Y. Yang, K. Farquhar, et al., "Surface Modification of Gd Nanoparticles With pH-Responsive Block Copolymers for Use as Smart MRI Contrast Agents," *American Chemical Society Applied Materials & Interfaces* 8 (2016): 5040–5050.

38. S. L. Canning, T. J. Neal, and S. P. Armes, "pH-Responsive Schizophrenic Diblock Copolymers Prepared by Polymerization-Induced Self-Assembly," *Macromolecules* 50 (2017): 6108–6116.

39. T. Sun, J. Zhu, M. Wang, et al., "A Glucosyl Triblock Copolymer: Synthesis and Its Injectable Thermo- and pH-Responsive Behaviours," *Royal Society of Chemistry Advances* 5 (2015): 24231–24238.

40. M. Hrubý, S. K. Filippov, and P. Štěpánek, "Smart Polymers in Drug Delivery Systems on Crossroads: Which Way Deserves Following?," *European Polymer Journal* 65 (2015): 82–97.

41. X. R. Shao, X. Q. Wei, X. Song, et al., "Independent Effect of Polymeric Nanoparticle Zeta Potential/Surface Charge, on Their Cytotoxicity and Affinity to Cells," *Cell Proliferation* 48 (2015): 465–474.

42. S. L. Anderson and K. C. Stylianou, "Biologically Derived Metal Organic Frameworks," *Coordination Chemistry Reviews* 349 (2017): 102–128.

43. O. Altintas, M. Artar, G. Ter Huurne, et al., "Design and Synthesis of Triblock Copolymers for Creating Complex Secondary Structures by Orthogonal Self-Assembly," *Macromolecules* 48 (2015): 8921–8932.

44. H. R. Allcock, Y. C. Song, and L. B. Steely, "New Amphiphilic Poly[Bis(2,2,2-Trifluoroethoxy)phosphazene]/Poly(Propylene Glycol) Triblock Copolymers: Synthesis and Micellar Characteristics," *Macromolecules* 39 (2006): 8334–8338.

45. P. Paik, A. Gedanken, and Y. Mastai, "Chiral-Mesoporous-Polypyrrole Nanoparticles: Its Chiral Recognition Abilities and Use in Enantioselective Separation," *Journal of Materials Chemistry* 20 (2010): 4085.

46. N. Greenfield and G. D. Fasman, "Computed Circular Dichroism Spectra for the Evaluation of Protein Conformation," *Biochemistry* 8 (1969): 4108–4116.

47. K. Matsuo, R. Yonehara, and K. Gekko, "Improved Estimation of the Secondary Structures of Proteins by Vacuum-Ultraviolet Circular Dichroism Spectroscopy," *Journal of Biochemistry* 138 (2005): 79–88.

48. J. Babin, J. Rodriguez-Hernandez, S. Lecommandoux, H. A. Klok, and M. F. Achard, "Self-Assembled Nanostructures From Peptide–Synthetic Hybrid Block Copolymers: Complex, Stimuli-Responsive Rod–Coil Architectures," *Faraday Discussions* 128 (2005): 179–192.

49. F. Chécot, A. Brûlet, J. Oberdisse, Y. Gnanou, O. Mondain-Monval, and S. Lecommandoux, "Structure of Polypeptide-Based Diblock Copolymers in Solution: Stimuli-Responsive Vesicles and Micelles," *Langmuir* 21 (2005): 4308–4315.

50. T. Luo, L. He, P. Theato, and K. L. Kiick, "Thermoresponsive Self-Assembly of Nanostructures From a Collagen-Like Peptide-Containing Diblock Copolymer," *Macromolecular Bioscience* 15 (2015): 111–123.

51. D. Priftis, L. Leon, Z. Song, et al., "Self-Assembly of α-Helical Polypeptides Driven by Complex Coacervation," *Angewandte Chemie International Edition* 54 (2015): 11128–11132.

52. S. W. Kang, Y. Li, J. H. Park, and D. S. Lee, "pH-Triggered Unimer/Vesicle-Transformable and Biodegradable Polymersomes Based on PEG-b-PCL–Grafted Poly(β-Amino Ester) for Anti-Cancer Drug Delivery," *Polymer (Guildf)* 54 (2013): 102–110.

53. L. R. Velatooru, C. B. Baggu, and V. R. Janapala, "Spatane Diterpinoid From the Brown Algae,Stoechospermum Marginatuminduces Apoptosis via ROS Induced Mitochondrial Mediated Caspase Dependent Pathway in Murine B16F10 Melanoma Cells," *Molecular Carcinogenesis* 55 (2016): 2222–2235.

54. R. Mancuso, R. Amuso, G. Grasso, et al., "Synthesis and Antibacterial Activity of Polymerizable Acryloyloxyalkyltriethyl Ammonium Salts," *ChemPlusChem* 82 (2017): 1235–1244.

55. M. Balouiri, M. Sadiki, and S. K. Ibnsouda, "Methods for In Vitro Evaluating Antimicrobial Activity: A Review," *Journal of Pharmaceutical Analysis* 6 (2016): 71.

56. W. Lu, T. Rades, J. Rantanen, H. K. Chan, and M. Yang, "Amino Acids as Stabilizers for Spray-Dried Simvastatin Powder for Inhalation," *International Journal of Pharmaceutics* 572 (2019): 118724.

57. J. Wang, B. Chen, D. Zhao, Y. Peng, R. X. Zhuo, and S. X. Cheng, "Peptide Decorated Calcium Phosphate/Carboxymethyl Chitosan Hybrid Nanoparticles With Improved Drug Delivery Efficiency," *International Journal of Pharmaceutics* 446 (2013): 205–210.

Supporting Information

Additional supporting information can be found online in the Supporting Information section.